THE INFLUENCE OF MICROSTRUCTURE ON FATIGUE CRACK INITIATION AND FATIGUE CRACK PROPAGATION IN Al-Mg-Si ALLOYS

W. Ruch* and V. Gerold*

The effect of microstructural features on the fatigue behaviour of a commercial and a pure alloy Al-1wt.%Mg-1wt.% Si has been studied in detail. The commercial alloy was obtained as (i) coarse grained and (ii) non-recrystallized fine grained version. Fatigue tests on notched specimens were undertaken in the peak aged condition. As a main result, both commercial modification showed a comparable fatigue life but substantial differences in crack initiation and propagation periods. The fatigue life of the coarse grained version could be improved if the notch was machined before the final heat treatment. The latter caused a fine-grained recrystallization area close to the notch improving the resistance against crack initiation.

INTRODUCTION

The total life time during fatigue generally can be divided into two regimes: one for crack initiation and another one for crack propagation. In the case of precipitation hardened alloys both regimes are influenced markedly by the microstructure of the material. Important microstructural features are second phase particles such as large inclusions (> 5 μm), small dispersoids (0.1 to 1 μm) and the strengthening precipitates (< 20 nm). The distribution of such particles can be influenced by manufacturing processes and heat treatments which may influence other microstructural parameters as grain size, degree of recrystallization and texture. Crack initiation during fatigue is promoted, for example, by microstructures which tend to develop an inhomogeneous deformation which is usually more pronounced in coarse grained material. On the other hand, the crack propagation rate of such cracks along slip bands may slow down in such material because of a high reversibility of slip in front of the crack tip as proposed by Hornbogen and Zum Gahr (1). In microstructures with a more homogeneous slip distribution, cracks will mainly nucleate at large inclusions. The resistance to fatigue crack initiation may be better than it is for inhomogeneously deforming microstructures, but the crack propagation resistance can be lower in this case. In the present paper the influence of different microstructures on fatigue properties will be studied in detail. For this purpose a commercial aluminium alloy has been manufactured in different ways resulting in different microstructures.

MATERIAL PREPARATION AND EXPERIMENTAL DETAILS

For the present investigation a pure (P) and a commercial (C) aluminium alloy containing 1 wt.% Mg and 1 wt.% Si have been selected. The commercial alloy contained also 0.8 wt.% Mn and 0.4 wt.% Fe. By using two different heat treatments before extruding the latter a coarse (CC) and a fine (CF) microstructure

*Max-Planck-Institut für Metallforschung, Institut für Werkstoffwissenschaften, Seestraße 92, D-7000 Stuttgart 1, Federal Republic of Germany

were obtained. All alloys were received as extruded bars with a cross section of 3 x 20 mm^2. After sample preparation but before machining the notch all specimens were solution treated for 10 min at 535°C followed by water quenching and ageing for 16 h at 160°C which led to the peak aged condition. All microstructures were investigated by light microscopy and transmission electron microscopy.

All three alloys showed large inclusions of Mg_2Si particles 5 to 20 μm in dimension which had an oval shape and were elongated in the extrusion direction. The commercial alloys CC and CF also contained large inclusions of another intermetallic phase enriched in Fe, Si and Mn. This second phase was larger in size and more blocky shaped than the former. Dispersoids in the size range 0.1 to 1 μm were observed only in the commercial alloys. They contained Mn and differed in their dispersion. Alloy CC showed a coarse dispersion with particle sizes of the order of 0.5 μm. These particles could not prevent recrystallization during extrusion. Therefore, large pancake shaped grains resulted with an average grain size of 400 μm. In contrast, alloy CF contained finely dispersed particles with an average size of 0.1 μm. The resulting grain structure was non-recrystallized with a 5 to 15 μm subgrain size. The absence of dispersoids in the pure alloy P resulted in a globular grain structure with an average size of 90 μm. Details of the microstructures and resulting mechanical properties are listed on Table 1.

TABLE 1 - Microstructures and Mechanical Properties for Alloys P, CC and CF

Alloy	P	CC	CF
Large inclusions	Mg_2Si, 5-10 μm	Mg_2Si, 5-10 μm; Fe,Si, Mn-rich, 10-20 μm	as CC
Dispersoids	-	0.5 μm	0.1 μm
Strengthening precipitates	coherent, needle shaped Mg_2Si-zones along<100>, about 20 nm long and 1-2 nm wide.		
Grain size (μm)	globular 90	pancake shaped 450/320	subgrains 5-15
Slip distribution	inhomogeneous very coarse	inhomogeneous coarse	homogeneous fine
UTS (MPa)	340	325	365
σ_y (MPa)	325	310	350
ε_f (%)	10	13	14

All microstructures were studied in the peak aged condition. The coherent nature of the strengthening precipitates promotes localized slip in deformation bands in all three cases because the precipitates are sheared during deformation (Dowling and Martin (2)). The dispersoids, however, which cannot be sheared by dislocations tend to have the reverse effect. Because of their fine distribution in alloy CF the resulting plastic deformation mode is quite homogeneous. In the alloy CC, however, the coarsely distributed dispersoids result in more concentrated slip in coarse slip bands. This slip inhomogeneity is still more pronounced in the pure alloy P where dispersoids are absent.

All specimens were machined to dimensions of 2.5 x 10 x 60 mm^3. After the final heat treatment different types of notches were machined into the specimens. For fatigue life and crack initiation studies a semicircular notch with 3 mm radius was made. The crack initiation was observed by light microscopy with a magnification of 200 or 400 x. The observable minimum crack size was 5 µm. For crack propagation studies a V-shaped notch with a depth of 2.0 mm was used. For a representative relationship between propagation rate and ΔK, 5 to 7 samples were necessary. All specimens were carefully polished to 1 µm diamond finish.

The fatigue experiments were performed with a mechanical testing machine under stress controlled pull-pull conditions (R = 0.1) in laboratory air using a frequency of 25 Hz. The stress amplitude in the following diagrams is defined as the difference between maximum and minimum stress values.

RESULTS AND DISCUSSION

Fatigue Life to Failure

Fig. 1 shows the Wöhler diagrams of the three investigated alloys. Surprisingly, no difference is observed between the diagrams of alloys CC and CF in spite of their quite different microstructures and slip behaviour. However, both fatigue lifes are about 4 to 5 times larger compared to the fatigue life of the pure alloy P.

Fatigue Crack Initiation

The number of cycles to crack initiation, N_i, as a function of the stress amplitude has been plotted on Fig. 2. N_i is defined as the number of cycles when a crack of 5 to 10 µm length could first be detected on the notch surface. On this figure, only the curves for alloys CC and CF are plotted because the crack initiation for alloy P occurs already after very few cycles in the whole stress amplitude region. Both curves for alloy CC and CF differ by a factor 2 in N_i. Obviously, the coarse structure CC is more susceptible to crack initiation than the fine structure CF.

The largest cracks during the initiation stage are formed in the pure alloy P. They nucleate either in persistent slip bands (PSBs) or at grain boundaries. The slip bands have the length of the grain diameter (90 µm) because there are no dispersoids hindering their development. The larger slip length and the coarse slip distribution result in high slip offsets on the surface leading to a fast crack nucleation. The nucleation at grain boundaries probably is caused by precipitation free zones (PFZs) adjacent to the boundary. A close inspection of intergranular fracture surfaces reveals fine dimples indicating strong local deformation in these zones. The third possible source for crack nucleation, namely the large Mg_2Si inclusions, does not play a role in this alloy as well as in the other ones.

In the alloy CC the length of the slip bands is smaller than in P due to

the presence of the coarsely distributed Mn-rich dispersoids. At high stress amplitudes ($\Delta\sigma$ > 120 MPa) the first cracks form again at PSBs on the surface as in alloy P. However, crack nucleation at grain boundaries is not observed in this case. One possible reason for this observation is the pancake shape of the grains which are elongated parallel to the stress axis. With decreasing stress amplitudes crack nucleation more and more is initiated at the large blocky inclusions of the intermetallic phase enriched in Fe, Mn and Si. At amplitudes $\Delta\sigma \leq$ 115 MPa they are the only nucleation source. This nucleation occurs by interface decohesion and not by fracture of the inclusion. The formed microcracks follow the path of PSBs into the matrix.

The third alloy CF deforms only homogeneously due to the highly dispersed very fine Mn-rich dispersoids. No slip lines or slip band cracking could be observed at all investigated stress amplitudes. Fatigue cracks always initiated at the larger type of inclusions as mentioned before. In this case the microcracks grow perpendicular to the loading axis in a non-crystallographic manner.

Fatigue Crack Propagation

The crack propagation behaviour of macrocracks for the three alloys can be seen on Fig. 3. The best overall fatigue crack growth resistance is observed for alloy CC. The rate dependence on the stress intensity amplitude ΔK can be approximated by a straight line in the log-log plot which results in an exponent of about 3.5 in the corresponding Paris Law. The points measured for the other commercial alloy CF are shifted to lower ΔK values by a factor 1.5 compared to alloy CC. The slope of the corresponding straight line has the same value as before. The result for the pure alloy P is given by an average straight line in order to avoid confusion. Its slope has a value of 5 which is much higher compared to the other cases.

Fracture surface examinations by scanning electron microscopy (SEM) gave the following results:

For the pure alloy P and for low ΔK values transgranular slip band cracking is mainly observed with coarse steps in the fracture surface. With increasing ΔK intergranular fracture becomes dominant. Very fine dimples on the intergranular fracture surface indicate plastic deformation in this region as already mentioned before. This change in the fracture mode can be explained by the varying size of the plastic zone in front of the crack tip. For small ΔK values this size is smaller than the grain size. Plastic deformation occurs mainly in the grain interior leading to PSB formation and softening in these bands due to destruction of precipitation particles (Vogel et al. (3)). Slip band cracking occurs as a result with a relatively high slip reversibility as suggested by Hornbogen and Zum Gahr (1). Therefore, resistance against crack propagation is improved leading to relative high ΔK values for low propagation rates. With increasing ΔK the plastic zone size is approaching the grain size. This leads to plastic deformation in the PFZs adjacent to the grain boundaries followed by intergranular fracture. This transition of the fracture mode with increasing ΔK may explain the larger slope of alloy P compared to the others.

For alloy CC the grain size is greater than the plastic zone size for ΔK values up to 16 $MNm^{-3/2}$. The fracture path is completely transgranular and follows the PSBs. At higher ΔK the fracture surface is showing regions with non-crystallographic appearance. At very high ΔK (> 20 $MNm^{-3/2}$) the crack is increasingly propagating by void coalescence caused by the large inclusions. The good crack propagation resistance of this alloy may be explained by the complete absence of grain boundary separation. This absence may be favoured by the anisotropy of the grain shape. In addition, the slip length in the grains

is limited by the existence of dispersoids which results only in low dislocation pile-ups at the grain boundary which are not able to fracture the boundary (Raymond and Martin (4)).

The fracture of alloy CF deforming homogeneously can be characterized by transgranular non-crystallographic crack surfaces in the whole range of ΔK. At high ΔK, fine striations frequently can be seen. The high crack propagation rate for this microstructure may be explained by the very homogeneous nature of deformation. Similar results have been obtained for other precipitation hardened alloys (Lindigkeit et al. (5)).

IMPROVING FATIGUE LIFE CONDITIONS

The preceding results on fatigue crack initiation and propagation are summarized schematically on Fig. 4. For the pure alloy P the whole life time is determined only by the crack propagation period since the nucleation period is restricted to the first few cycles of the experiment. For the commercial alloy C the total fatigue life N_f is the same for its both versions CC and CF. However, the fatigue initiation and propagation periods are quite different. For the CC version about 60% of the life time is used up for crack initiation whereas more than 95% is needed for the CF version.

This result may lead to the idea to improve the fatigue property of the commercial alloy C in such a way that the microstructure CF is used in areas where crack initiation is expected while the bulk of the material consists of microstructure CC leading to a higher resistance against crack propagation. This case is sketched on Fig. 4 as "CC+CF" microstructure.

Such a case has been studied accidentally at the beginning of this research. In these preliminary experiments flat specimens were used with a drilled center hole as a crack nucleation site. The final heat treatment was carried out afterwards which caused recrystallization in an area close to the center hole. For the CC specimens the resulting grain size was about 50 µm as sketched on Fig. 5. The CF specimens also show recrystallized grains of 50 to 100 µm size in the notch root. All samples were fatigued to failure in a similar way as described before. Surprisingly, the Wöhler curve of the CC version resulted in a higher fatigue life than the CF version (Fig. 6). Both curves differed by a factor 2 in fatigue life. Now, these results can be explained in the way described above. The recrystallized area at the surface of the hole improves the resistance against crack nucleation for the CC specimens, whereas for the CF specimens there is either a reverse effect or no effect at all. Additional experiments on the same sample geometry are in progress to prove the validity of this explanation.

The authors are obliged to Prof. W. Gruhl and Dr. G. Scharf, Vereinigte Aluminium-Werke AG (VAW), Bonn, for their suggestion to investigate the two versions of the commercial alloy and for providing the extruded material.

REFERENCES

1. Hornbogen, E., and Zum Gahr, K.-H., 1976, Acta Met., 24, 581
2. Dowling, J.M., and Martin, J.W., 1973, Proc. 3rd Conf. on Strength of Metals and Alloys, p. 170, Cambridge Univ. Press, London
3. Vogel, W., Wilhelm, M. and Gerold, V., 1982, Acta Met., 30, 21
4. Raymond, P.V., and Martin, J.W., 1979, Z. Metallkde., 70, 80
5. Lindigkeit, J., Gysler, A., and Lütjering, G., 1981, Met. Trans. A, 12A, 1613

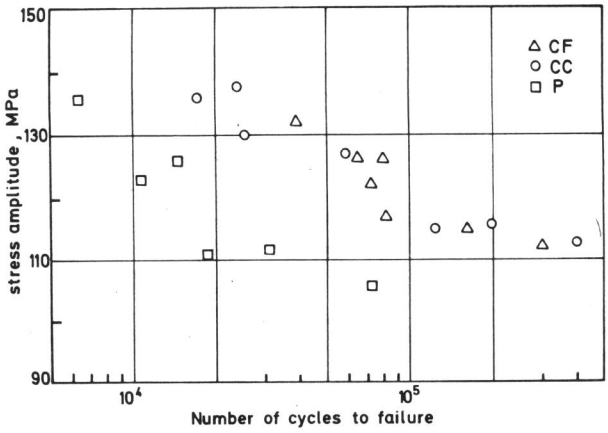

Figure 1 Wöhler diagrams for notched specimens of the three alloys P, CC and CF

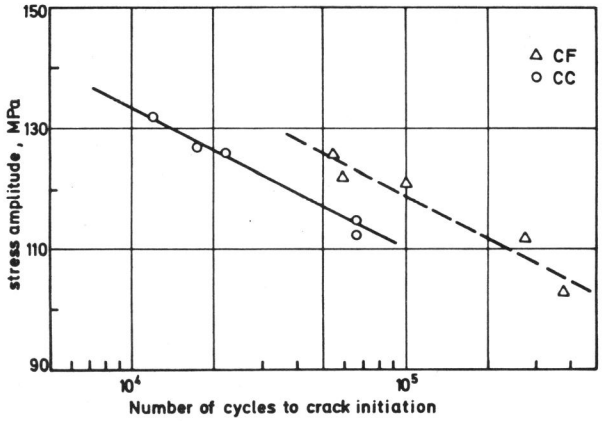

Figure 2 Crack initiation as a function of the stress amplitude for alloys CC and CF

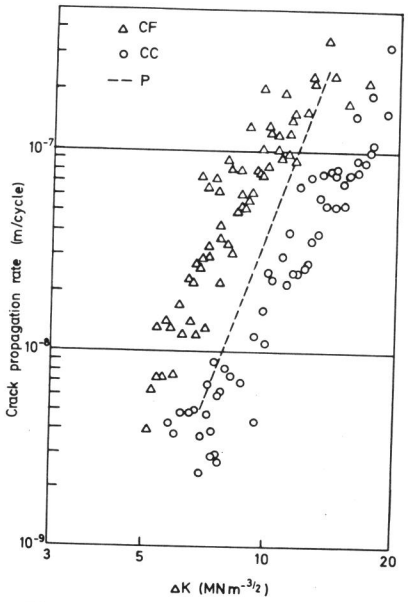

Figure 3 Crack propagation rates for alloys P, CC and CF

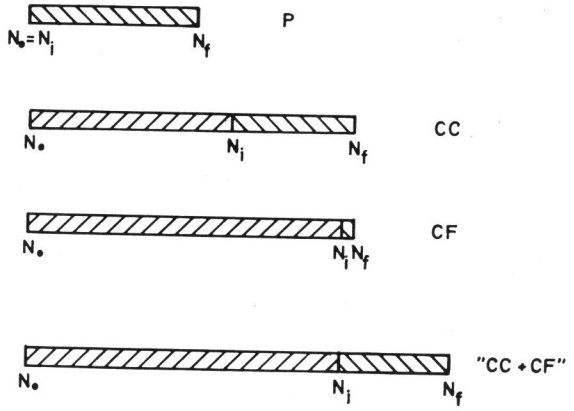

Figure 4 Crack nucleation and propagation periods during life time

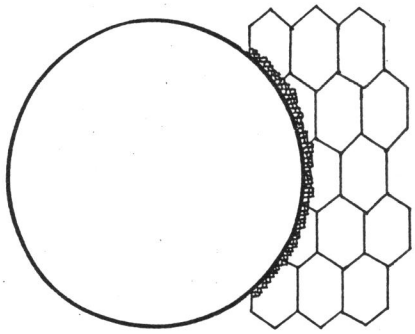

Figure 5 Recrystallized area at the drilled hole of CC specimen

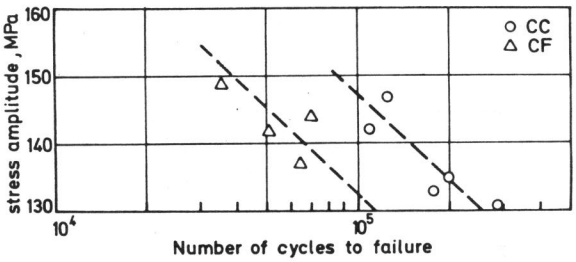

Figure 6 Wöhler diagram for samples CC and CF with a center hole